ACS OMEGA

http://pubs.acs.org/journal/acsodf

Article

# Comparative Analysis of the Hydrogen Bond Vibrations of Ice XII

Xiao-Qing Yuan, Xu-Hao Yu, Xu-Liang Zhu, Xue-Chun Wang, Xiao-Yan Liu, Jing-Wen Cao, Xiao-Ling Qin, and Peng Zhang*

Cite This: *ACS Omega* 2022, 7, 2970−2974

Read Online

ACCESS | Metrics & More | Article Recommendations | Supporting Information

**ABSTRACT:** It is difficult to theoretically study the vibrational spectrum of hydrogen-disordered ice XII compared with its hydrogen-ordered counterpart, ice XIV. We constructed a 24-molecule supercell of ice XII to mimic its real structure. We focused on hydrogen bond (HB) vibrational modes in the translation band using first-principles density functional theory (DFT). Our simulated results were in good agreement with inelastic neutron scattering experiments. We found that the optical vibrational modes of HBs are composed of three main components. These are cluster vibrations in the lowest-frequency region, four-bond HB vibrations in the highest-frequency region, and two-bond modes in between. Although the experimentally recorded curve of ice XII is smooth in the translation region, our results support the proposal that two types of intrinsic HB vibrational modes are common in the ice family.

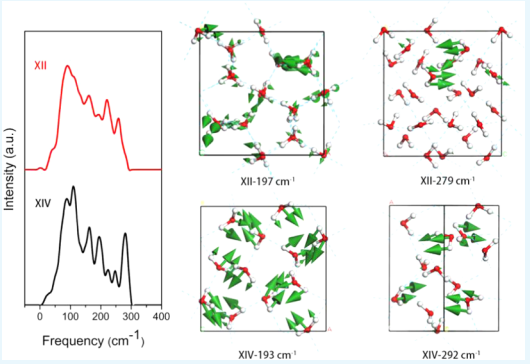


## 1. INTRODUCTION

Water is a valuable natural resource and plays a significant role in life. Experiments have confirmed that ice exists in more than 20 solid phases and new conformations are constantly being discovered.[1] These conformations differ in their crystal or amorphous structures.[2−13] Most ice phases exist in pairs of hydrogen-ordered or disordered arrangements, and each member of a pair can be converted to the other under specific conditions. Ice XIV and ice XII is one such hydrogen-ordered/disordered pair, having the same sublattice structure of oxygen.[9] Ice XII was discovered in 1998 by Lobban et al. Under conditions of 260 K and 0.55 GPa.[14] In 2000, Koza et al. found that when ice Ih was compressed to 77 K, it could be transformed into ice XII, although it was later confirmed to pass through a high-density amorphous intermediate phase.[15,16] Kohl's experiments showed that ice XII could be formed by subjecting ice Ih to a sudden pressure drop at 77 K.[17] In 2004, Andersson and co-authors reported an expanded range of external conditions (temperature and pressure) under which this ice phase could exist.[18,19] In 2006, Salzmann et al. successfully achieved the transformation of ice XII to ice XIV through hydrochloric acid catalysis, and later the transformation of ice XIV to XII under heated conditions was observed.[20,21]

Because ice XII is a hydrogen-disordered phase, it is difficult to analyze its vibrational spectrum using the lattice dynamics method. However, based on our previous study on its hydrogen-ordered counterpart ice XIV,[22] herein, we compare and discuss the vibrational modes of the HBs of ice XII and attempt to explain the far-infrared vibrational curve, especially with regards to the HBs.

## 2. RESULTS AND DISCUSSION

The calculated phonon density of states (PDOS) of ice XII and ice XIV and the inelastic neutron scattering (INS) data of ice XII in the translation band are shown in Figure 1.[16,22] The INS spectrum of ice XII was obtained by Koza et al. using a neutron spectrometer, the TOSCA-ISIS, at the Rutherford-Appleton Laboratory.[16] The best results were obtained below 1000 cm$^{-1}$ due to a large Debye−Waller factor at the higher-energy transfer ranges of this instrument. Thus, we only plot the molecular translation and libration bands in Figure 1. The PDOS of ice XII is in good agreement with the INS spectrum. Ignoring the impact of scattering cross sections of different elements and multiphonon scattering, INS gathers all phonons throughout the first Brillouin zone so that the INS signals are theoretically almost exactly proportional to the PDOS. Therefore, we can directly compare the INS spectrum with the PDOS curve. In the INS spectrum, there is an absorption band from 161.2 to 306.2 cm$^{-1}$ (i.e., from 20 to 38 meV). This matches the band from 167 to 280 cm$^{-1}$ obtained in this study. The lower-frequency sharp peak within this band corresponds to acoustic branch phonons. In the INS spectrum, the libration band starts at 59 meV (475.5 cm$^{-1}$) and corresponds to the peak at 502.8 cm$^{-1}$ in the PDOS curve.[16]

**Received:** October 26, 2021
**Accepted:** December 29, 2021
**Published:** January 10, 2022

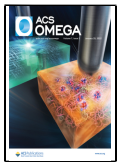





https://doi.org/10.1021/acsomega.1c06000
*ACS Omega* 2022, 7, 2970−2974

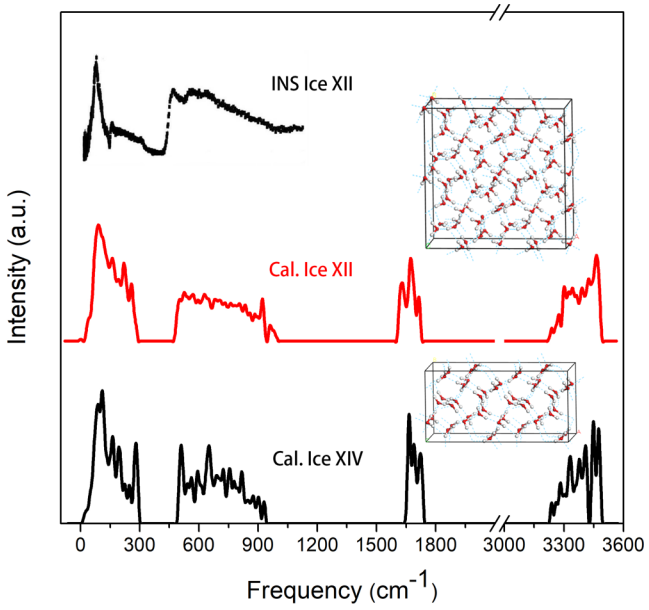


**Figure 1.** Comparison of the simulated spectra of ice XII and ice XIV. The top curve is the INS experimental spectrum of ice XII. The middle curve in red is the PDOS of ice XII, while the bottom curve is the PDOS of ice XIV. A 96-molecule supercell of ice XII and a 48-molecule supercell of ice XIV are inserted.

We previously reported the vibrational spectrum of the ice XII's hydrogen-ordered counterpart, ice XIV.[22] The simulated PDOS curve is plotted in Figure 1 for comparison. It is obvious that most of the peaks of the two spectra are homologous with each other. Due to its hydrogen-ordered structure, the model of ice XIV is a 12-molecule primitive cell, which has $12 \times 3 \times 3 - 3 = 105$ optical normal modes. Thus, the calculated spectrum shows more pronounced peaks than that of ice XII. There are 24 molecules in the supercell of ice XII. The number of calculated optical normal modes is $24 \times 3 \times 3 - 3 = 213$ and all of the modes are nondegenerate. The overlapping of the peaks gives rise to a smooth spectral curve.

In 1989, Li et al. found two characteristic vibrational peaks in the molecular translation band of the INS spectrum of ice Ih.[23] However, the origin of these two peaks is under continuous debate.[24−31] In our previous studies, we found two kinds of intrinsic HB vibrational modes in hydrogen-ordered ice Ic.[32] Later, this phenomenon was also observed in ices XIV, XVI, XVII, VII, VIII, XVI, VI, and others.[22,33−39] According to the Bernal−Fowler rules, each water molecule forms an HB with four adjacent water molecules in all ice phases, and this forms a local tetrahedral structure.[40,41] We used the ideal structure of hydrogen-ordered ice Ic as the basis to analyze the lattice dynamics process.

If we regard the water molecule as a point mass and take the oxygen atom as the center of mass, the unit cell is similar to that of a diamond. A primitive cell contains only two atoms. Under the harmonic approximation, the number of vibrational normal modes of HBs would be $2 \times 3 - 3 = 3$. Thus, we obtain three degenerate frequencies, which vibrate in three orthogonal directions (see ref 30 for details). The force matrix of lattice vibration is

$$\phi\alpha\beta\begin{pmatrix}1 & 1'\\ \mathrm{i} & \mathrm{i}'\end{pmatrix} = \left(\frac{\partial^2}{\partial \mathrm{u}_\alpha\begin{pmatrix}1\\ \mathrm{i}\end{pmatrix}\partial \mathrm{u}\beta\begin{pmatrix}1'\\ \mathrm{i}'\end{pmatrix}}\right)_0 = \begin{pmatrix} \frac{4}{3}k & 0 & 0 & -\frac{4}{3}k & 0 & 0 \\ 0 & \frac{4}{3}k & 0 & 0 & -\frac{4}{3}k & 0 \\ 0 & 0 & \frac{4}{3}k & 0 & 0 & -\frac{4}{3}k \\ -\frac{4}{3}k & 0 & 0 & \frac{4}{3}k & 0 & 0 \\ 0 & -\frac{4}{3}k & 0 & 0 & \frac{4}{3}k & 0 \\ 0 & 0 & -\frac{4}{3}k & 0 & 0 & \frac{4}{3}k \end{pmatrix} \quad (1)$$

We obtain

$$\omega_1 = \omega_2 = \omega_3 = \sqrt{\frac{1}{m}\left(\frac{8k}{3}\right)} \quad (2)$$

However, the existence of hydrogen atoms breaks the local tetrahedral symmetry. Based on a first-principles simulation, we obtain two vibrational frequencies, consisting of one strong mode and two weak degenerate modes.[32] That is, there are two force constants.

Then, we have

$$\begin{Bmatrix} \omega_s = \sqrt{\frac{1}{m}\left(\frac{8k_s}{3}\right)} \\ \omega_w = \sqrt{\frac{1}{m}\left(\frac{8k_w}{3}\right)} \end{Bmatrix} \quad (3)$$

where $\omega_s$ is the strong vibrational frequency, while $\omega_w$ is the weak frequency. According to the simulation of the ideal model of Ic, the wavenumbers of the two HB vibrations are $\omega_s$ = 320.76 $cm^{-1}$ and $\omega_w$ = 229.96 $cm^{-1}$.[32] Therefore, the ratio of the two frequencies is

$$\frac{\omega_s}{\omega_w} = \frac{320.76}{229.96} \approx 1.4 \approx \sqrt{2} \quad (4)$$

That is

$$\frac{k_s}{k_w} = 2 \quad (5)$$

Thus, the force constant of the strong HB mode is twice that of the weak mode. These two intrinsic HB modes in the translation region correspond to the two peaks recorded in the INS experiments. Our previous investigations on ideal ice Ic have revealed that for the strong mode, each molecule vibrates along the H−O−H angle bisector against four neighbors. The four HBs involved vibrate together, and this is called the four-bond mode. For the weak vibrations, each molecule vibrates along two HBs, while the other two HBs remain static. Therefore, the corresponding force constant is smaller and this


https://doi.org/10.1021/acsomega.1c06000
ACS Omega 2022, 7, 2970−2974

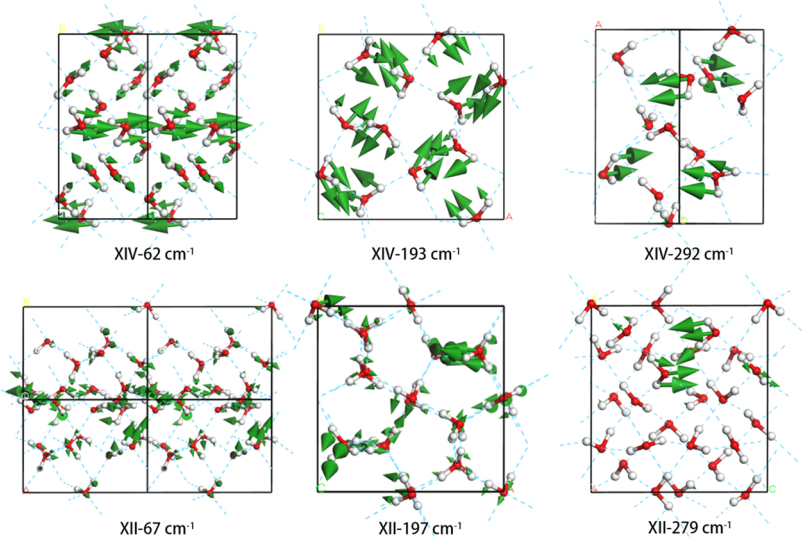


**Figure 2.** Top three modes are typical HB vibrations of ice XIV in the translation zone, and the bottom three modes are the corresponding HB vibrations of ice XII.

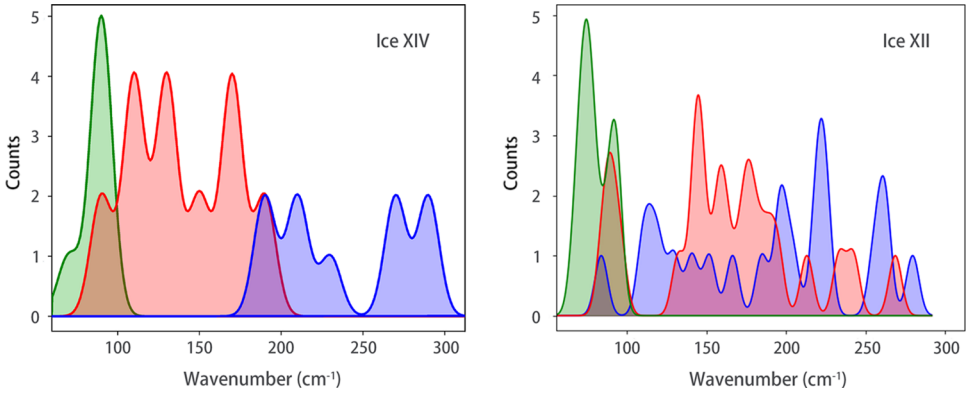


**Figure 3.** Comparison between ice XIV and ice XII showing the distributions of partial vibrational modes. The green curve shows the cluster vibrations, the red curve shows the two-bond vibrations, and the blue curve shows the four-bond vibrations.

is known as the two-bond mode. We have previously proven that this rule applies to ice XIV. In this study, we focus on the translation band to reveal the HB vibrations in ice XII.

Figure 2 shows three typical HB vibrational modes of ice XII compared with three modes of ice XIV. In our previous work on ice XIV, we identified a two-bond vibration and a four-bond vibration at 193 and 292 $cm^{-1}$, respectively.[22] The image of the vibration at 292 $cm^{-1}$ shows some molecules stretching toward the H−O−H angle bisector, while the vibration at 193 $cm^{-1}$ shows some molecules rocking or wagging along the direction of HBs. Although it is not clearly observable in the figure, we found four-bond modes at 279 $cm^{-1}$ and two-bond modes at 197 $cm^{-1}$ in ice XII (please see the videos from the Supporting file). However, from Figure 1, one can see two separate main peaks in ice XIV (around 280 and 160 $cm^{-1}$), while the curve for ice XII in the 130−300 $cm^{-1}$ range is smoother. Due to the hydrogen-disordered structure of ice XII, the vibrational modes are not clearly distinct and the boundary between them is blurred. As there are $24 \times 3 - 3 = 69$ nondegenerate normal modes in the translation band, many adjacent modes couple together to show a smooth curve.

In the lower-frequency region of the translation band of ice XV, Whale et al. found peaks corresponding to "rigid network modes".[42] In ice XV, these modes are non-HB vibrations that consist of relative vibrations between two sublattices. There are no such modes in ice XII as all of the molecules are connected via HBs. However, one can see that some clusters vibrate in the lower-frequency frequency band of ice XII. This involves many molecules bound together that vibrate collectively. The modes at 62 $cm^{-1}$ of ice XIV and at 67 $cm^{-1}$ of ice XII are presented in Figure 2 (please see the dynamic process from the Supporting file). The number of participating HBs in the cluster vibrational mode is less, while the mass of the cluster is greater, resulting in lower vibrational energy.

We classified the PDOS in the translation band into three categories corresponding to the three modes using a self-compiled program, as shown in Figure 3.[43] It can be seen that the three modes of ice XIV are separated clearly. The region of the four-bond mode (in blue) is from 180 to 300 $cm^{-1}$ and the two-bond mode (in red) is from 90 to 180 $cm^{-1}$. The green curve, which has the lowest frequency, shows the cluster vibrational modes. However, the boundaries between the mode types in ice XII are not as clear. Some of the four-bond modes and two-bond modes overlap. We attribute this phenomenon to three causes: (1) the deformation of the tetrahedral structure caused by disordered hydrogen; (2) the center of mass being positioned at oxygen; and (3) limited accuracy of the self-compiled program. Regardless of these


https://doi.org/10.1021/acsomega.1c06000
ACS Omega 2022, 7, 2970−2974

factors, the trends of ice XIV and XII are consistent. When all of the modes overlap, the two types of HB vibrational peaks merge into a smooth curve, as shown in the INS results in Figure 1. However, from our results, we can conclude that the HB vibrations of ice XIV and XII in this region are composed of distinct four-bond modes, two-bond modes, and cluster modes.

## 3. CONCLUSIONS

To study the vibrational spectrum of hydrogen-disordered ice XII, we constructed a 24-molecule supercell, calculated its PDOS curve, and analyzed its vibrational normal modes. As the calculated curve was consistent with the INS spectrum, we focused on comparing the translation band with that of its hydrogen-ordered counterpart, ice XIV. Theoretically, we deduced that the energy ratio of the strong and weak intrinsic HB vibrations is $\sqrt{2}$, which has been proposed as a general rule among the ice family.

Due to the hydrogen-disordered structure, all of the normal modes in a supercell are nondegenerate. Thus, there are many coupled vibrational modes in between the cluster, two-bond, and four-bond modes. Based on a simple algorithm, we found that the boundary between two-bond and four-bond modes is blurry. However, the trend is consistent with ice XIV. Although the INS spectrum presented an almost completely smooth curve in the region of the translation band, we can conclude that the optical modes are composed of three distinct components. These are the cluster vibrations in the lowest-frequency region, the four-bond HB vibrations in the highest-frequency region, and the two-bond modes in between.

## 4. COMPUTATIONAL METHOD

Due to the hydrogen-disordered structure of ice XII, there is no periodically repeating unit. To mimic a real structure, we employed the program GenIce to create a supercell containing 24 molecules, and the hydrogens were randomly added according to the Bernal−Fowler rules.[40,44] Based on the first-principles DFT, we used the CASTEP software module for geometric optimization and phonon calculations.[45] Based on our previous experience, the generalized gradient approximation (GGA) exchange−correlation functional RPBE was used, as the electron density has a large gradient change.[33−39,46] The convergence tolerance value of energy and the self-consistent field was set to $1 \times 10^{-9}$ eV/atom. The energy cutoff was 830 eV and the *k*-point mesh was $2 \times 2 \times 2$ under 0.55 GPa of pressure. We used a self-compiled program to classify the molecular vibrational modes to facilitate the HB analysis (please see the source code from the Supporting file).[43]

## ■ ASSOCIATED CONTENT

### Supporting Information

The Supporting Information is available free of charge at https://pubs.acs.org/doi/10.1021/acsomega.1c06000.

Source code for distinguishing the mode type of hydrogen bonds (PDF)

Demonstration of the typical vibrational mode of ice XII-67 (MP4)

Demonstration of the typical vibrational mode of ice XII-197 (MP4)

Demonstration of the typical vibrational mode of ice XII-279 (MP4)

## ■ AUTHOR INFORMATION


### Corresponding Author

**Peng Zhang** − *School of Space Science and Physics, Shandong University, Weihai 264209 Shandong, China;* orcid.org/0000-0002-1099-6310; Email: zhangpeng@sdu.edu.cn

### Authors

**Xiao-Qing Yuan** − *School of Space Science and Physics, Shandong University, Weihai 264209 Shandong, China*

**Xu-Hao Yu** − *School of Space Science and Physics, Shandong University, Weihai 264209 Shandong, China*

**Xu-Liang Zhu** − *School of Space Science and Physics, Shandong University, Weihai 264209 Shandong, China*

**Xue-Chun Wang** − *School of Space Science and Physics, Shandong University, Weihai 264209 Shandong, China;* orcid.org/0000-0001-7839-3842

**Xiao-Yan Liu** − *School of Space Science and Physics, Shandong University, Weihai 264209 Shandong, China*

**Jing-Wen Cao** − *School of Space Science and Physics, Shandong University, Weihai 264209 Shandong, China;* orcid.org/0000-0002-3226-3281

**Xiao-Ling Qin** − *School of Space Science and Physics, Shandong University, Weihai 264209 Shandong, China*

Complete contact information is available at: https://pubs.acs.org/10.1021/acsomega.1c06000


### Notes

The authors declare no competing financial interest.

## ■ ACKNOWLEDGMENTS

The authors are grateful to the National Natural Science Foundation of China for financial support (grant no. 11075094). The numerical calculations were performed on the supercomputing system at the Supercomputing Center, Shandong University, Weihai.

## ■ REFERENCES


(1) Yamane, R.; Komatsu, K.; Gouchi, J.; Uwatoko, Y.; Kagi, H.; et al. Experimental evidence for the existence of a second partially-ordered phase of ice VI. *Nat. Commun.* **2021**, *12*, No. 1129.

(2) Bertie, J. E.; Whalley, E. Optical Spectra of Orientationally Disordered Crystals. II. Infrared Spectrum of Ice Ih and Ice Ic from 360 to 50 cm−1. *J. Chem. Phys.* **1967**, *46*, 1271−1284.

(3) Bertie, J. E.; Calvert, L. D.; Whalley, E. Transformations of Ice II, Ice III, and Ice V at Atmospheric Pressure. *J. Chem. Phys.* **1963**, *38*, 840−846.

(4) Kuhs, W. F.; Finney, J. L.; Vettier, C.; Bliss, D. V. Structure and hydrogen ordering in ices VI, VII, and VIII by neutron powder diffraction. *J. Chem. Phys.* **1984**, *81*, 3612−3623.

(5) Whalley, E.; Heath, J. B. R.; Davidson, D. W. Ice IX: An Antiferroelectric Phase Related to Ice III. *J. Chem. Phys.* **1968**, *48*, 2362−2370.

(6) Tajima, Y.; Matsuo, T.; Suga, H. Phase transition in KOH-doped hexagonal ice. *Nature* **1982**, *299*, 810−812.

(7) Hirsch, K. R.; Holzapfel, W. B. Effect of high pressure on the Raman spectra of ice VIII and evidence for ice X. *J. Chem. Phys.* **1986**, *84*, 2771−2775.

(8) Lobban, C.; Finney, J. L.; Kuhs, W. F. The structure of a new phase of ice. *Nature* **1998**, *391*, 268−270.

(9) Salzmann, C. G.; Radaelli, P. G.; Hallbrucker, A.; Mayer, A. E.; Finney, J. L. The Preparation and Structures of Hydrogen Ordered Phases of Ice. *Science* **2006**, *311*, 1758−1761.

(10) Salzmann, C. G.; Radaelli, P. G.; Mayer, E.; Finney, J. L. Ice XV: A new thermodynamically stable phase of ice. *Phys. Rev. Lett.* **2009**, *103*, No. 105701.

(11) Falenty, A.; Hansen, T. C.; Kuhs, W. F. Formation and properties of ice XVI obtained by emptying a type sII clathrate hydrate. *Nature* **2014**, *516*, 231−233.
(12) Del Rosso, L.; Celli, M.; Ulivi, L. New porous water ice metastable at atmospheric pressure obtained by emptying a hydrogen-filled ice. *Nat. Commun.* **2016**, *7*, No. 13394.
(13) Salzmann, C. G.; Loveday, J. S.; Rosu-Finsen, A.; Bull, C. L. Structure and nature of ice XIX. *Nat. Commun.* **2021**, *12*, No. 3162.
(14) Lobban, C.; Finney, J. L.; Kuhs, W. F. The structure of a new phase of ice. *Nature* **1998**, *391*, 268−270.
(15) Koza, M. M.; Schober, H.; Hansen, T.; Tolle, A.; Fujara, F. Ice XII in its second regime of metastability. *Phys. Rev. Lett.* **2000**, *84*, 4112−4115.
(16) Koza, M. M.; Schober, H.; Parker, S. F.; Peters, J. Vibrational dynamics and phonon dispersion of polycrystalline ice XII and of high-density amorphous ice. *Phys. Rev B.* **2008**, *77*, No. 104306.
(17) Kohl, I.; Mayer, E.; Hallbrucker, A. Ice XII forms on compression of hexagonal ice at 77 K via high-density amorphous water. *Phys. Chem. Chem. Phys.* **2001**, *3*, 602−605.
(18) Andersson, O.; Johari, G. P. Spontaneous transformation of water's high-density amorph and a two-stage crystallization to ice VI at 1 GPa: A dielectric study. *J. Chem. Phys.* **2004**, *120*, 11662−11671.
(19) Andersson, O.; Johari, G. P.; Suga, H. An ice phase of lowest thermal conductivity. *J. Chem. Phys.* **2004**, *120*, 9612−9617.
(20) Salzmann, C. G.; Radaelli, P. G.; Hallbrucker, A.; Mayer, E.; Finney, J. L. Spontaneous transformation of water's high-density amorph and a two-stage crystallization to ice VI at 1 GPa: A dielectric study. *Science* **2006**, *311*, 1758.
(21) Köster, K. W.; Fuentes-Landete, V.; Raidt, A.; Seidl, M.; Gainaru, C.; Loerting, T.; Böhmer, R. Dynamics enhanced by HCl doping triggers 60% Pauling entropy release at the ice XII−XIV transition. *Nat. Commun.* **2015**, *6*, No. 7349.
(22) Zhang, K.; Zhang, P.; Wang, Z. R.; Zhu, X. L.; Lu, Y. B.; Guan, C. B.; Li, Y. DFT Simulations of the Vibrational Spectrum and Hydrogen Bonds of Ice XIV. *Molecules* **2018**, *23*, No. 1781.
(23) Li, J. C.; Ross, D. K.; Howe, L.; Hall, P. G.; Tomkinson, J. Inelastic incoherent neutron scattering spectra of single crystalline and polycrystalline ICE Ih. *Phys. B* **1989**, *156−157*, 376−379.
(24) Li, J. C.; Ross, D. K. Evidence for two kinds of hydrogen bond in ice. *Nature* **1993**, *365*, 327−329.
(25) Li, J. C. Inelastic neutron scattering studies of hydrogen bonding in ices. *J. Chem. Phys.* **1996**, *105*, 6733−6755.
(26) Li, J. C.; Kolesnikov, A. I. J. Neutron spectroscopic investigation of dynamics of water ice. *Mol. Liq.* **2002**, *100*, 1−39.
(27) Klotz, S.; Strässle, Th.; Salzmann, C. G.; Philippe, J.; Parker, S. F. Incoherent inelastic neutron scattering measurements on ice VII: Are there two kinds of hydrogen bonds in ice? *Europhys. Lett.* **2005**, *72*, 576−582.
(28) He, X.; Sode, O.; Xantheas, S. S.; Hirata, S. Second-Order Many-Body Perturbation Study of Ice Ih. *J. Chem. Phys.* **2012**, *137*, No. 204505.
(29) Zhang, P.; Tian, L.; Zhang, Z. P.; Shao, G.; Li, J. C. Investigation of the hydrogen bonding in ice Ih by first-principles density function methods. *J. Chem. Phys.* **2012**, *137*, No. 044504.
(30) Zhang, P.; Han, S. H.; Yu, H.; Liu, Y. A calculating proof on hydrogen bonding in ordinary ice by the first-principles density functional theory. *RSC Adv.* **2013**, *3*, 6646−6649.
(31) Zhang, P.; Wang, Z.; Lu, Y. B.; Ding, Z. W. The normal modes of lattice vibrations of ice XI. *Sci. Rep.* **2016**, *6*, No. 29273.
(32) Yuan, Z. Y.; Zhang, P.; Yao, S. K.; Lu, Y. B.; Yang, H. Z.; Luo, H. W.; Zhao, Z. J. Computational Assignments of Lattice Vibrations of Ice Ic. *RSC Adv.* **2017**, *7*, 36801−36806.
(33) Zhu, X. L.; Yuan, Z. Y.; Jiang, L.; Zhang, K.; Wang, Z. R.; Luo, H. W.; Gu, Y.; Cao, J. W.; Qin, X. L.; Zhang, P. Computational Analysis of Vibrational Spectrum and Hydrogen Bonds of Ice XVII. *New J. Phys.* **2019**, *21*, No. 043054.
(34) Gu, Y.; Zhu, X. L.; Jiang, L.; Cao, J. W.; Qin, X. L.; Yao, S. K.; Zhang, P. Comparative Analysis of Hydrogen Bond Vibrations in Ice VIII and VII. *J. Phys. Chem. C.* **2019**, *123*, 14880−14883.
(35) Wang, Z. R.; Zhu, X. L.; Jiang, L.; Zhang, K.; Luo, H. W.; Gu, Y.; Zhang, P. Investigations of the Hydrogen Bonds and Vibrational Spectra of Clathrate Ice XVI. *Materials* **2019**, *12*, No. 246.
(36) Qin, X. L.; Zhu, X. L.; Cao, J. W.; Jiang, L.; Gu, Y.; Wang, X. C.; Zhang, P. Computational Analysis of Exotic Molecular and Atomic Vibrations in Ice XV. *Molecules* **2019**, *24*, No. 3115.
(37) Cao, J. W.; Zhu, X. L.; Wang, H. C.; Qin, X. L.; Yuan, X. Q.; Wang, X. C.; Yu, J. L.; Ma, X. T.; Li, M. M.; Zhang, P. A Strategy for the Analysis of the Far-Infrared Vibrational Modes of Hydrogen-Disordered Ice V. *J. Phys. Chem. C.* **2021**, *125*, 7913−7918.
(38) Wang, X. C.; Zhu, X. L.; Gu, Y.; Wang, H. C.; Qin, X. L.; Cao, J. W.; Yu, X. H.; Yuan, X. Q.; Zhang, P. Comparative Analysis of Hydrogen-Bonding Vibrations of Ice VI. *ACS Omega* **2021**, *6*, 14442−14446.
(39) Yu, X. H.; Qin, X. L.; Dong, X. T.; Cao, J. W.; Zhu, X. L.; Wang, H. C.; Sun, Y. J.; Xu, Z. X.; Zhang, P. Studies of Hydrogen Bond Vibrations of Hydrogen-Disordered Ice Ic. *Crystals* **2021**, *11*, No. 668.
(40) Bernal, J. D.; Fowler, R. H. A theory of water and ionic solution, with particular reference to hydrogen and hydroxyl ions. *J. Chem. Phys.* **1933**, *1*, 515−548.
(41) Qin, X. L.; Zhu, X. L.; Cao, J. W.; Wang, H. C.; Zhang, P. Investigation of hydrogen bond vibrations of ice. *Acta Phys. Sin.* **2021**, *70*, No. 146301.
(42) Whale, T. F.; Clark, S. J.; Finney, J. L.; Salzmann, C. G. DFT-assisted interpretation of the Raman spectra of hydrogen-ordered ice XV. *J. Raman Spectrosc.* **2013**, *44*, 290−298.
(43) Zhu, X. L.; Cao, J. W.; Qin, X. L.; Jiang, L.; Gu; Wang, H. C.; Liu, Y.; Kolesnikov, A. I.; Zhang, P. Origin of two distinct peaks of ice in the THz region and its application for natural gas hydrate dissociation. *J. Phys. Chem. C* **2020**, *124*, 1165−1170.
(44) Matsumoto, M.; Takuma, Y.; Hideki, T. GenIce: Hydrogen-disordered ice generator. *J. Comput. Chem.* **2018**, *39*, 61−64.
(45) Clark, S. J.; Segall, M. D.; Pickard, C. J.; Hasnip, P. J.; Probert, M. I. J.; Refson, K.; Payne, M. C. First principles methods using CASTEP. *Z. Kristallogr. - Cryst. Mater.* **2005**, *220*, 567−570.
(46) Hammer, B.; Hansen, L. B.; Norskov, J. K. Improved adsorption energetics within density-functional theory using revised Perdew- Burke-Ernzerhof functionals. *Phys. Rev. B* **1999**, *59*, 7413−7421.


https://doi.org/10.1021/acsomega.1c06000
*ACS Omega* 2022, 7, 2970−2974